J. Fluid Mech. (1990), *vol.* 212, *pp.* 241–262
Printed in Great Britain

Hydrodynamic interactions in directional solidification

By STEPHEN H. DAVIS
Department of Engineering Sciences and Applied Mathematics, Northwestern University, Evanston, IL 60208, USA

(Received 14 June 1989)

A binary liquid undergoes unidirectional solidification. The one-dimensional steady state is susceptible to morphological instability that causes the solid/liquid interface to change from a planar state to a cellular pattern. This paper examines the effects on this transition of volume-change convection, buoyancy-driven convection or forced flows. It emphasizes how flows alter stability limits, create scale and pattern changes in morphology, and create, through coupling, new instabilities. Emphasis is placed on the physical mechanisms of the interactions.

1. Introduction

The solidification of a liquid involves a complex interplay of many physical effects. The solid/liquid interface is an active free boundary on which latent heat is liberated during phase transformation. This heat is conducted away from the interface through the solid and/or liquid establishing thermal boundary layers near the interface. Further, across the interface the density changes, say, from ρ_L to ρ_S. Thus, if $\rho_S > \rho_L$, so that the material shrinks upon solidification, there is a flow induced toward the interface from 'infinity'.

If the liquid is not pure, but contains solute, then preferential rejection or incorporation of solute generally occurs at the interface. For example, if there is a single solute present and its solubility is smaller in the (crystalline) solid than it is in the liquid, the solute will be rejected at the interface. This rejected material of concentration c is diffused away from the interface through the solid and/or liquid setting up concentration boundary layers near the interface. The thermal- and concentration-boundary-layer distributions determine in part whether there exist *morphological instabilities* in solidification.

If the solidification process occurs in a gravitational field, the thermal and solutal gradients induce buoyancy-driven convection that is known to greatly affect the interfacial patterns and hence the solidification microstructures that are present in the solidified material (see e.g. Rosenberger 1979, p. 2).

The present paper concerns various aspects of *directional solidification*. Figure 1 shows a typical experimental configuration in which two constant-temperature sources are fixed in a laboratory frame. A binary liquid fills the region between two parallel, closely spaced plates forming a Hele-Shaw cell. When the plates are laid across the temperature sources, the material solidifies at a position where the local temperature equals the melting (or solidification) temperature T_I; the interface is planar in this static configuration. The plates are now pulled at constant speed V downward, toward the solid. After transients have disappeared, the solid/liquid interface remains stationary in the laboratory frame, since it is 'pinned' at $T = T_I$,

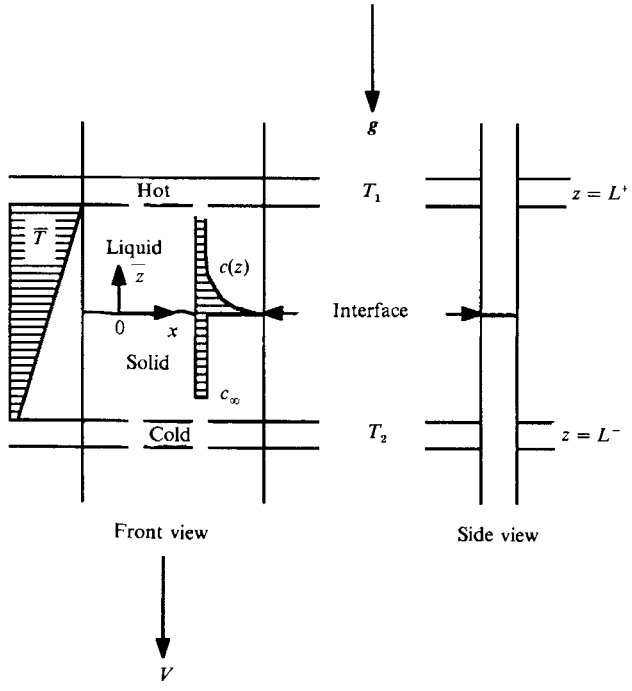

FIGURE 1. Configuration for directional solidification in a Hele-Shaw cell. The mean position of the interface is $z = 0$ and the temperature T is linear in the 'frozen-temperature approximation'.

yet the material is *continuously* solidified at rate V. (T_I now differs somewhat from the T_1 in the static state since $T_I = T_1(c_1)$.) This configuration is widely used for detailed experiments with organic binary liquids since the material is transparent and the thin-domain geometry allows visual/optical viewing of the interface. To be sure, the growth of single crystals commercially or in natural contexts involves the growth in fully three-dimensional geometries of opaque metallic or semiconductor materials.

It is known on the bases of theory (Mullins & Sekerka 1964) and of experiment (Rutter & Chalmers 1953; Boettinger, *et al.* 1984; Trevedi, Sekhar & Seetharaman 1989) that the interface remains planar during solidification of binary liquids at non-zero values of the pulling speed V until a first critical value V_c is attained; see figure 2(*a*). Near V_c, nearly two-dimensional steady cells will appear, as shown in figure 2(*b*), and these deepen as V is increased (see figure 2*c*). As V is increased further, there is a dendritic transition in which deep cells develop side branches, as shown in figure 2(*d*). Finally, there is a second critical value of V, $V = V_A$, the absolute stability limit; as $V \to V_A$, these dendritic structures fade to cells, and the cells fade further until the planar interface regains stability. The article by Langer (1980) gives an overview of these events and also discusses solidification phenomena that occur in other contexts.

The 'pure' morphological instability in unidirectional solidification is diffusive in nature, being driven by the adverse gradient of solute concentration c at the interface as will be explained in §2. The onset of cellular structure creates lateral variations in c in the liquid and when solute is rejected, its concentration is elevated in the troughs of the cells. When the grooves between cells, shown in figure 2(*c*), are deep, the solute is trapped there; the large path lengths from the root to the bulk liquid above make longitudinal diffusion very slow compared to the rate of growth at the tip. The solidified material will inherit these non-uniformities, a set of high-c stripes parallel

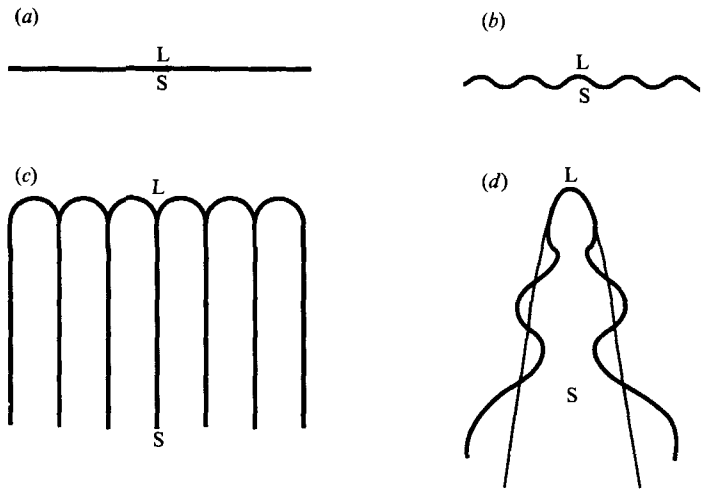

FIGURE 2. A rough sketch of interface shapes: (*a*) the plane interface, (*b*) shallow cells, (*c*) deep cells, (*d*) the dendrite.

to the growth direction. The stripes extend downward until a new phase (not shown) is encountered.

When the liquid is flowing, the solute distribution is rearranged. It may be homogenized and so delay the morphological instability. However, if the flow is unsteady, say time periodic, the temperature oscillation will be accompanied by oscillations in c at the interface. These oscillations cause both modulation of the boundary-layer thicknesses and of the growth speed V. These in turn will create variations in concentration in the solid, resulting in striations, bands of concentration variations, perpendicular to the growth direction. Oscillatory motion in the liquid is one of the most frequent causes of crystalline inhomogeneities (Rosenberger 1979, p. 2).

In the present paper we investigate the effects of hydrodynamics in directional solidification. We find that the flow can alter the critical conditions for the onset of morphological instability. It can create scale and pattern changes in the morphology. It can create, through coupling, new instabilities that pre-empt the old and give new criteria for morphological changes. In §2 we outline the 'pure' morphological-instability problem. In §3 we detail the types of interactions that can occur. In §4 we discuss volume-change convection ($\rho_L \neq \rho_S$) and the important solute-transport mechanisms. In §5 we examine coupled morphological/buoyant-convective instabilities. In §6 we examine forced flows imposed on interfaces and highlight flow-induced morphological instabilities. In §7 we examine flows on developed cells or dendrites. Section 8 gives a closing discussion of some issues omitted earlier.

Directional solidification, actually unidirectional solidification, simulates one-dimensional phase change with control of the temperature field and pulling rate V. It thus allows for the study of small-scale phenomena in controlled phase transformation. One can study the growth of single crystals, the initiation of cellular instabilities, and the transition to dendritic structure. There is an important category of phenomena that are large scale, ones that involve large gradients, multidirectional solidification, turbulent 'double-diffusive' convection, and whole beds of dendrites. These occur in casting processes and in geological settings. Many of these topics are discussed in the article by Huppert (1990).

2. Morphological instabilities (MI)

Figure 1 shows a directional-solidification cell in which a binary liquid undergoes phase transformation at melting temperature T_1. Convection is absent and for simplicity of presentation the system is taken to be two-dimensional. We further invoke the 'frozen-temperature approximation' (Langer 1980) which gives the temperature T in the solid and liquid permanently by

$$T = T_0 + Gz, \tag{2.1}$$

where G is the (imposed) temperature gradient, z is the coordinate along the temperature gradient and T_0 is a reference temperature.

Form (2.1) is a good approximation when (i) the latent heat L liberated at the interface is conducted away much faster than the interface advances (small Stefan number), (ii) the solute diffusion is much slower than the thermal conduction (so that on small lengthscales solute effects are rate limiting), and (iii) the thermal conductivities, k_S and k_L of the solid and liquid, respectively, are taken to be equal. The details of the thermal field are relatively unimportant in directional solidification since the liberated heat conducts predominantly downward through the (cold) solid and, perhaps, the sidewalls, but only slightly affects the conditions in the liquid.

Given that the temperature field (2.1) is passive, it is only the solute concentration c in the liquid that can be perturbed. If the coordinate system moves with the planar interface, the diffusion equation has the form

$$c_t - Vc_z = D\nabla^2 c, \tag{2.2}$$

where subscripts denote partial differentiation and D is the diffusivity of the solute in the liquid.

The instability is driven at the interface $z = h(x,t)$ where jump conditions are obtained using the assumption of local thermodynamic equilibrium.

At the interface, the solute, assumed dilute, is rejected causing a discontinuity in c across the interface. This is measured by the segregation (or distribution) coefficient k,

$$k = c^-/c^+, \tag{2.3}$$

taken from a linearized phase diagram. Since rejection is taking place, $0 \leqslant k < 1$, and the concentration, c^+, on the liquid side exceeds that, c^-, on the solid side.

The temperature T_1 on the interface is given by the Gibbs–Thompson equation

$$T_1 = mc^+ + T_M\left[1 + 2H\frac{\gamma}{L}\right], \tag{2.4a}$$

where

$$2H = \nabla\cdot\{[1+|\nabla h|^2]^{-\frac{1}{2}}\nabla h\}. \tag{2.4b}$$

Here, $m, m < 0$, is the slope of the liquidus, and mc^+ represents the alteration of the melting point due to the presence of solute, the *constitutional undercooling*. The surface energy γ enters the *capillary undercooling* term in which γ/L multiplies $2H$, twice the mean curvature of the interface; the melting point is lowered when the interface is concave toward the solid.

If we combine (2.1) and (2.4), we obtain

$$T_0 - T_M + Gh = mc^+ + T_M\frac{\gamma}{L}2H. \tag{2.5}$$

Finally, there is the solute balance across the interface,

$$(c^+ - c^-)(V + h_t) = -D(c_z^+ - c_x^+ h_x). \tag{2.6}$$

If we combine (2.3) and (2.6), we have

$$(1-k)\,c^+(V+h_t) = -D(c_z^+ - c_x^+ h_x). \tag{2.7}$$

Given that the linear profile (2.1) for the temperature is used and confining our attention to lengthscales much smaller than L^+, the top of the cell, $z = L^+$, can be replaced by infinity; we then have that

$$c \to c_\infty \quad \text{as } z \to \infty. \tag{2.8}$$

System (2.2), (2.5), (2.7) and (2.8) represents the simplest model of 'pure' morphological instabilities, which we abbreviate as MI. It assumes that the densities ρ_S and ρ_L are equal so that convection due to volume changes is absent. It assumes that body forces are absent so that buoyancy-driven convection is also absent. It ignores diffusion in the solid and invokes the 'frozen-temperature approximation'. It is written in two dimensions and is a special case of that posed by Mullins & Sekerka (1964).

There is a steady *basic state* that consists of a planar interface,

$$\bar{h} \equiv 0, \tag{2.9a}$$

a constant concentration c_S in the solid, a concentration boundary layer in the liquid

$$\bar{c} = c_\infty\left(1 + \frac{1-k}{k}\mathrm{e}^{-z/\delta_c}\right), \tag{2.9b}$$

where

$$T_0 - T_M = \frac{m}{k}c_\infty, \tag{2.9c}$$

and

$$\delta_c = D/V. \tag{2.10}$$

Notice that by using (2.3), (2.8) and (2.9*b*) evaluated at $z = 0$,

$$c^- = c_\infty \equiv c_S, \quad c^+ = c_S/k \equiv c_L. \tag{2.11}$$

In actuality, the basic state has exponential structure in both c and T, with the concentration-boundary-layer thickness δ_c and that for temperature $\delta_T = \kappa/V$, where κ is the thermal diffusivity in the liquid. However, by assumption $\kappa \gg D$, and the thermal profile becomes the linear one given by (2.1).

The instability of the planar basic state was explained first by Tiller *et al.* (1953) and a full linear-stability theory, including the effects of surface energy, was first given by Mullins & Sekerka (1964). Coriell, McFadden & Sekerka (1985) give a fine survey of past results. The mechanism can be explained (Langer 1980) by the use of figure 3, which shows the basic state, $\bar{c}$ and $\bar{h}$, and an initial disturbance of the system in the form of an interfacial corrugation. A bump of solid pushes its front into a higher temperature environment and thus tends to melt back; the temperature distribution is stabilizing. A bump of solid is concave downward and so by the Gibbs–Thomson effect has its local melting point decreased. By (2.4) the bump tends to melt back; surface energy is stabilizing. A bump of solid will compress the isopycnals in the liquid above it. Thus, the local concentration gradient is increased. By (2.6) the local growth rate will increase. The material in front of the bump will freeze faster and the interfacial growth will tend to run away; the concentration gradient G_c at the interface drives the instability.

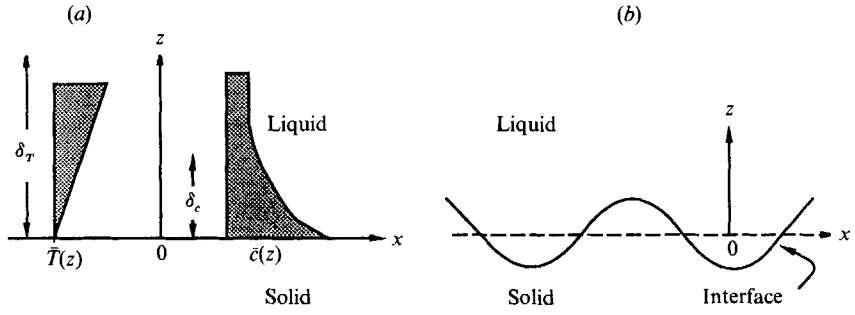

FIGURE 3. (a) The basic-state fields. (b) The corrugated interface.

We can calculate G_c from (2.9) and find that

$$G_c = -\frac{1-kc_\infty}{k}\frac{V}{D}. \tag{2.12}$$

We see that $|G_c|$ increases with increasing pulling rate V, and with increased concentrations c_∞ of solute present. It decreases the faster the diffusion removes the rejected solute from the interfacial region. When $k \to 0$, all the solute is rejected from the solid and $|G_c|$ is large. When $k \to 1$, there is no rejection, $c_S = c_L$, and hence no morphological instability.

The stability index can be expressed as the ratio M,

$$M = \frac{mG_c}{G}. \tag{2.13}$$

The liquid is constitutionally undercooled if $M > 1$. When surface energy is present, the condition for instability (Mullins & Sekerka 1964) is $M > M_c$ where $M_c \geqslant 1$.

The linear-stability-theory results of Mullins & Sekerka (1964) can be represented in the 'frozen-temperature approximation' by figure 4, here for the case of succinonitrile-acetone (SCN-A) which has $k_S/k_L \approx 1.009$. For a given temperature gradient G, one fixes c_∞ and increases V. If $c_\infty < c_\infty^*$, the system is below the critical concentration c_∞^* and the planar state is stable. If $c_\infty > c_\infty^*$, then there is a first critical speed V_c, beyond which the basic state is unstable to steady (two-dimensional) cells. According to linear theory, there is a second critical value, the absolute-stability limit V_A, above which the basic state restabilizes.

Figure 4(a) indicates that the neutral curve splits into two portions. The dashed curve, nearly the whole lower branch, corresponds to subcritical bifurcation to two-dimensional cells, as obtained by the first weakly nonlinear theory, that of Wollkind & Segel (1970). The solid curve, indicates supercritical bifurcation, and occupies the whole upper branch and a small section of lower branch.

When the 'frozen-temperature' approximation is relaxed, the critical conditions on the lower branch are only slightly altered. However, the position of the transition point separating subcritical/supercritical bifurcation behaviour can move substantially. Alexander, Wollkind & Sekerka (1986) performed such an analysis in two dimensions. Figure 4(b) shows the neutral curve for SCN-A, analogous to that in figure 4(a). Figure 4 is taken from Merchant & Davis (1989b) who use these to argue that shallow cells in MI can be produced in laboratory experiments to give the linear and weakly nonlinear theories quantitative tests.

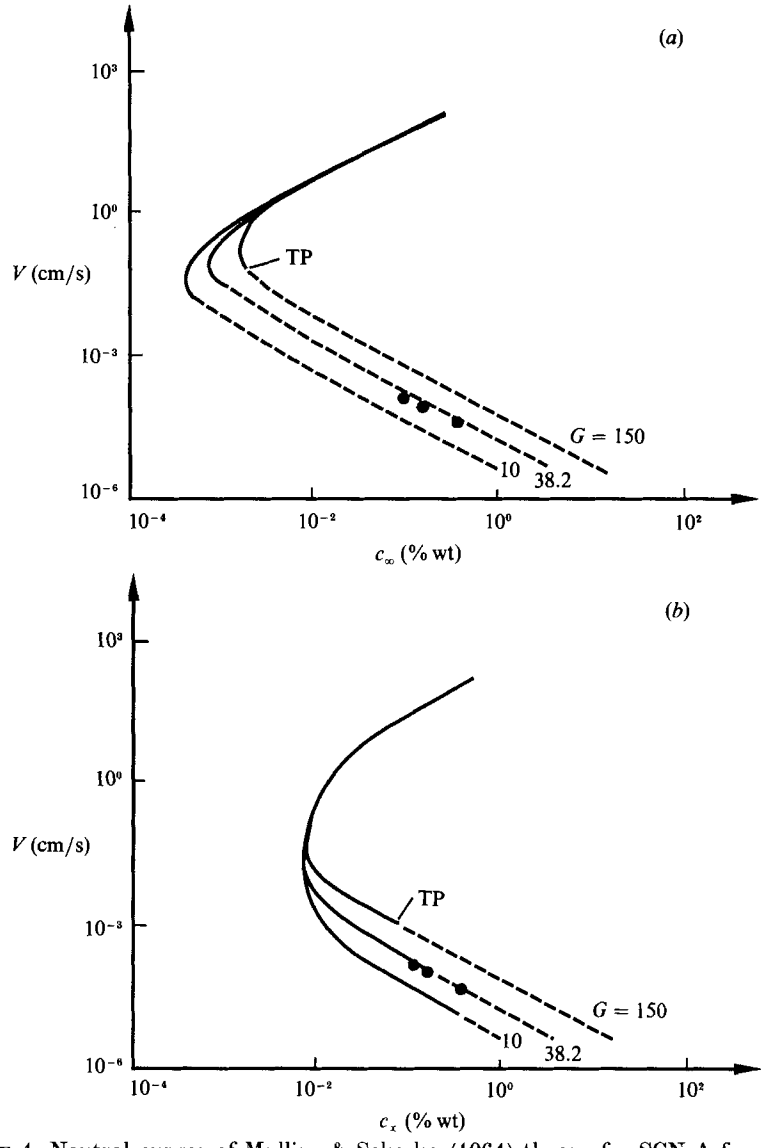

FIGURE 4. Neutral curves of Mullins & Sekerka (1964) theory for SCN-A for various G (K/cm), taken from Merchant & Davis (1989*b*), subject to (*a*) the 'frozen-temperature approximation', (*b*) the full effects of differing thermal conductivities and latent heat. Solid (dashed) lines correspond to supercritical (subcritical) bifurcation and TP denotes the transition point that separates these (according to Wollkind & Segel 1970 and Alexander *et al.* 1986). The open circles correspond to experimental results of Eshelman & Trevedi (1987). The nose of a given curve has coordinates (c_∞^*, V^*). Note that the lower branch away from the nose is given by $M \approx 1$.

Let l_c be the capillary length,

$$l_c = \frac{\gamma T_M k}{Lm(k-1)c_\infty}. \tag{2.14}$$

For large undercooling, $mG_c \gg G$, (well beyond the lower linear-stability boundary) the wavelength λ of the cells is determined by solute rejection and surface energy so that (Langer 1980)

$$\lambda/\delta_c \propto (l_c/\delta_c)^{\frac{1}{2}}. \tag{2.15a}$$

Since l_c is normally much smaller than δ_c, λ is usually much smaller than δ_c. When the system is near the lower linear-stability boundary, $mG_c \approx G$, the speeds are lower and the wavelengths are larger,

$$\lambda/\delta_c \propto (l_c/\delta_c)^{\frac{1}{3}}. \tag{2.15b}$$

The 'frozen-temperature' approximation is based on $k_S/k_L = 1$ and the inequalities $\delta_c \ll L^+$, $\delta_c \ll \delta_T$, where L^+ is the distance from the interface to the heat source as shown in figure 1. When the disturbance wavelength λ is large enough that it is comparable with $\min(\delta_T, L^+)$, then the curvature of the temperature profile may become important. Long waves are, indeed, preferred in MI in two cases: (i) on the lower branch if one allows the distribution coefficient k to be small, $\lambda_c \sim k^{-\frac{1}{4}}$ as shown by Sivashinsky (1983); (ii) on the upper branch if one approaches the absolute-stability limit, $V \to V_A$ (Mullins & Sekerka 1964). In both these cases care must be exercised when using the local linear form for the temperature.

There have been numerous studies of nonlinear cellular behaviour in addition to those of Wollkind & Segel (1970) and Alexander *et al.* (1986). Sriranganathan, Wollkind & Oulton (1983) and Wollkind, Sriranganathan & Oulton (1984) sought weakly nonlinear three-dimensional states but these are unstable unless extra physical effects are included. Ungar & Brown (1984*a*, *b*) and Ungar, Bennett & Brown (1985) studied deep cells and their two-dimensional secondary bifurcations in spatially periodic boxes using finite-element simulations. McFadden, Boisvert & Coriell (1987) used finite-difference simulation for the Al–Cr system, $k > 1$, and found stable hexagonal nodes. Merchant & Davis (1989*c*) studied two-dimensional bifurcations at $c_\infty \approx c_\infty^*$, and find multiple solutions and isolated solutions as functions of k_S/k_L; latent heat is neglected.

Sivashinsky (1983) studied the lower branch for $k \to 0$ and obtained a weakly nonlinear evolution equation that displays subcritical bifurcation. This was extended to include latent-heat effects by Novick-Cohen & Sivashinsky (1986). Brattkus & Davis (1988*a*) examined the long-wave instabilities near $V = V_A$ and derived a strongly nonlinear evolution equation. When this was specialized to small-amplitude two-dimensional disturbances, supercritical bifurcation was found. When three-dimensional disturbances were allowed, all two-dimensional states were found to become unstable and stable hexagonal nodes were found for both $k < 1$ and $k > 1$. Riley & Davis (1990) examined the long-wave evolution for $k \to 0$ but far from $mG_c = G$ and found a new strongly nonlinear evolution equation intermediate between those of Sivashinsky and Brattkus/Davis that tracks the transition in two dimensions between subcritical and supercritical bifurcation.

3. Interactions of hydrodynamics and morphology

When one attempts to grow single crystals, the state of pure diffusion rarely exists. Usually flow is present in the melt; it may be created by direct forcing or it may be due to the presence of convection. Brown (1988) gives a broad survey of the processing configurations and the types of flows that occur.

There are many examples of forced flows. The crystal may be rotated to erase non-axially symmetric thermal effects, but it creates a von Kármán swirl flow. The use of microgravity environments for the growth of crystals suppresses major buoyancy effects but the lurching of the spacecraft creates transient accelerations, g-jitter, that stir the liquid.

There are three types of convection that can occur in the liquid. (i) If the density of the liquid and solid are different, then bulk flows in the liquid are driven normal to the interface; this is volume-change convection, which is present even in Space. (ii) There is buoyancy-driven convection created by density gradients. In binary liquids, the double-diffusive convection can be steady when Rayleigh numbers exceed critical values or at arbitrary Rayleigh numbers owing to the presence of, say, heat losses at the sidewalls of the container. If the Rayleigh numbers are high enough, the steady convection can become unstable and, perhaps, unsteady. This is often the case in metallic or semiconductor materials which have very small Prandtl numbers. (iii) When fluid–fluid interfaces are present, as in the case of containerless processing by float-zone methods or the reprocessing of surfaces by lasers, steep temperature and concentration gradients on these interfaces can drive steady thermo-soluto-capillary convection. If these steady flows become unstable, unsteady states can occur.

All of the above-mentioned flows are in a sense accidental or at any rate unintentional. They cannot be prevented or else are present, as in the case of the swirl, because the rotation is necessary for other reasons. There can also be intentionally imposed flows. In the 1960's Hurle suggested that rather than crystal growers bemoaning the presence of convection as a source of crystal non-uniformities, they should try to 'design' natural convection (or forced flows) that will homogenize the solute boundary layer at the interface. In effect this would decrease the local gradient $|G_c|$ enough to eliminate the possibility of morphological instabilities. This attractive possibility has motivated a good deal of work on the coupling of flow and morphology.

If one entertains the possibility of interactions between morphology and, say, convection, one can imagine several modes of interaction. (i) If the solid and liquid have different densities, the interface drives a convective flow. We examine this in volume-change convection in §4. This discussion also serves as a vehicle for identifying the principal modes of solute transport in directional solidification. (ii) If one solidifies upward, as shown in figure 1, and if the solute rejected has lower density than the melt, then liquid is stably stratified thermally but unstably stratified solutally. Thus, there can be convective as well as morphological instabilities. There is the possibility that these can occur simultaneously and thus be strongly coupled. We examine these in §5. (iii) If the instabilities do not couple tightly at their onset, then one or the other dominates. In §6 we examine how morphological instabilities are affected by an existing flow in the liquid. Here we discover that the presence of the flow creates a coupled instability in the interface, a flow-induced morphological instability. (iv) The other extreme is one in which there is an existing morphology, say a set of finite-amplitude cells or dendrites, and one imposes upon this a fluid flow. One asks how the growth of the cellular field is altered by the flow. This will also be briefly discussed in §7. Finally, in §8 we shall discuss more general issues, such as when the model we have outlined may be unreliable, what other physics may need to be included in the models, and the need for quantitative experimentation.

4. Volume-change convection

The interface at $z = h(x, t)$ is the site of a phase transformation in which the liquid of density ρ_L changes to solid of density ρ_S. Morphological changes are driven by solute rejection there and in addition, if $\rho_L \neq \rho_S$, the interface drives a convective flow. For example the lead–tin alloy shrinks upon solidification, $\rho_S/\rho_L \approx 1.05$, and a

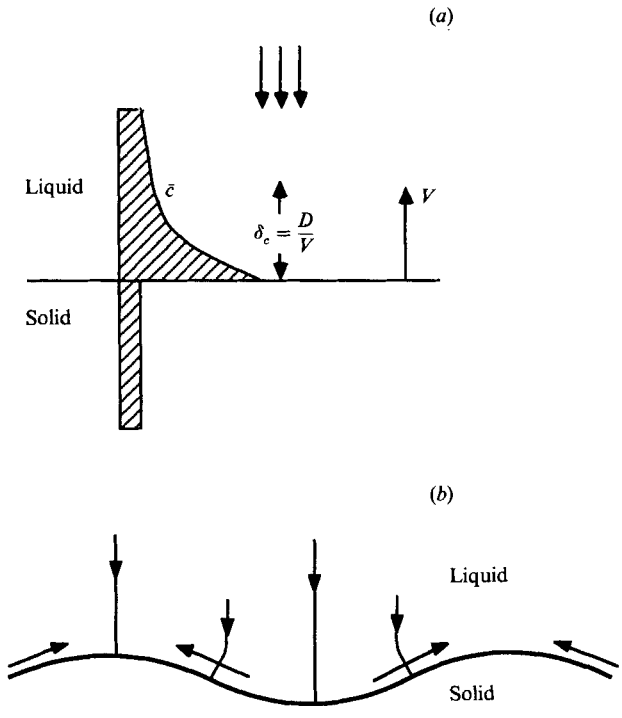

FIGURE 5. Transport mechanisms in volume-change convection for $\rho_S > \rho_L$: (*a*) boundary-layer alteration, (*b*) lateral transport.

weak flow from 'infinity' is generated in order to conserve mass. Silicon alloys expand upon solidification, $\rho_S/\rho_L \approx 0.91$, and the generated flow is from the interface to 'infinity'.

The governing system of §2 must be augmented by the Navier–Stokes and continuity equations and supplemented by boundary conditions on the velocity at infinity and at the interface. Since the interface is solid, the no-slip condition holds,

$$\boldsymbol{v}\cdot\boldsymbol{\tau} = 0 \quad \text{on} \quad z = h(x,t), \tag{4.1}$$

where $\boldsymbol{v} = (u,w)$ is the velocity in the liquid and $\boldsymbol{\tau}$ is the unit tangent vector to the interface. The mass balance across the interface becomes

$$(\rho_L - \rho_S)(V + h_t) = \rho_L(w - uh_x - h_t) \quad \text{on} \quad z = h(x,t). \tag{4.2}$$

When $\rho_L = \rho_S$, the interface is impermeable to flow, but when $\rho_L \neq \rho_S$, it acts as a porous surface that produces or consumes liquid at the rate required by the volume changes.

The linear theory for morphological instability with volume-change convection was done by Caroli *et al.* (1985*b*). The following explanation is a variant of theirs. Consider the case of shrinkage, $\rho_S > \rho_L$, as shown in figure 5(*a*). There are two competing effects that are present.

On the one hand the flow from infinity will cause the concentration boundary layer of thickness $\delta_c = D/V$ to be compressed so that the local gradient $|G_c|$ is increased. As discussed in §2, this will enhance the morphological instability through what we can term *boundary-layer alteration*. Thus, shrinkage is destabilizing, while expansion is stabilizing.

On the other hand consider the result of an initial corrugation of the interface as shown in figure 5(*b*). Since the interface is a no-slip surface, all streamlines cross the interface normally. At the crest or trough the streamlines are vertical but elsewhere they are curved. The curvature is accompanied by transverse velocities that, for $\rho_S > \rho_L$, carry the solute from the trough to the crests, as shown; this flow homogenizes the solute and decreases $|G_c|$. (Note that the 'pure' MI leads to excess solute in the troughs.) Thus, for the case of shrinkage, the induced *lateral transport* of solute is stabilizing.

Caroli *et al.* (1985*b*) found that low solidification speeds V, which correspond to thick concentration boundary layers, promote destabilization by shrinkage since the boundary-layer alteration is more effective than is lateral transport. At high speeds V, the opposite is the case.

Brattkus (1988) took another point of view by comparing different materials. Materials with small segregation coefficient k reject nearly all their solute. From (2.12) we see that $|G_c|$ is monotonic in k and Brattkus showed that systems with small k are destabilized when compared to the constant-density case; the reverse is true in materials with moderate k. This switch-over in effect with material properties is important to understand since many experiments for convenience substitute transparent organics for metallics; such a switch may also switch the influence of volume-change convection.

Clearly, volume-change convection has small effects if $(\rho_L - \rho_S)/\rho_L$ is small. It should only be of importance when other modes of convection are absent or else of very small magnitude. Such would be the case in a microgravity environment in Space. It might also be important in the deep roots between cells as shown in figure 2(*c*) where dimensions are small and where diffusion is very slow.

5. Coupled morphological/convective instabilities

Consider the directional solidification of a binary liquid in which the front moves vertically upward as shown in figure 1. The rejected-solute profile gives not only the possibility of morphological instability, but also the possibility of buoyancy-driven convective instability. If the solute is of low density, the steady basic state consists of a 'heated-from-above' temperature field and an unstably stratified concentration field. Thus, there can be a double-diffusive Bénard instability on a semi-infinite domain containing an exponentially decaying concentration profile and a (locally) linear temperature field.

The linear stability theory for $\rho_L = \rho_S$ has been examined in great detail (Coriell *et al.* 1980; Hurle, Jakeman & Wheeler 1982, 1983; Coriell 1984). Such theories give results typified by figure 6 showing, for fixed G and V, the mean solute concentration c_∞ versus wavenumber $a = 2\pi/\lambda$; here c_∞ is used as the bifurcation parameter. There are two coexisting neutral curves, one for the 'pure' convective mode and one for the 'pure' morphological. Typically, the critical wavenumbers $a_c^{(C)}$ and $a_c^{(M)}$ for the two are widely separated, with the convective mode of much longer scale. In the figure, $a_c^{(M)}/a_c^{(C)} \approx 6.5$ so that there is a large-scale convective flow with a small-scale morphology. As V is increased the lengthscale δ_c in the Rayleigh number decreases. Thus, as V is increased, the convective curve rises while the morphological curve falls.

At a specific value of V, the critical c_∞ of both modes coincide, giving the possibility of a coupled instability. The bifurcation theory (Jenkins 1985; Caroli *et al.* 1985*a*), however, shows that the wavelength disparity, mentioned above, leads to only a very weak coupling between the instabilities. This conclusion, however, is

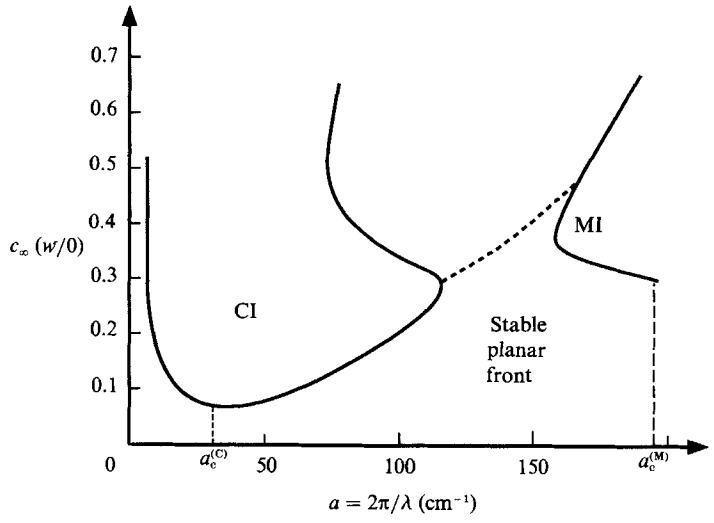

FIGURE 6. Neutral curves for Pb–Sn with $V = 30$ μm/s and $G = 200$ K/cm for upward solidification with the rejection of low-density solute. The convective instabilities (CI) and MI have preferred wavenumbers $a_c^{(C)}$ and $a_c^{(M)}$, respectively. Solid (dashed) curves denote steady (time-periodic) instability. Curves are taken from Coriell *et al.* (1980).

based upon the examination of only a small set of material systems, mainly lead–tin and SCN–Ethanol (Schaefer & Coriell 1982). Clearly, if the linear-theory critical values of c_∞ are common, and if $a_c^{(M)} = a_c^{(C)}$, then the two-dimensional problem has a codimension-two bifurcation structure and there is the possibility that strong interactions of the two modes would be possible; the appearance of secondary oscillations might then occur. More general interactions could also give rise to oscillations; an example is $a_c^{(M)}/a_c^{(C)} = 2$. Riley & Davis (1989*a*) have undertaken a systematic study of such possibilities for both these cases over wide classes of solutes, solvents and their material properties. Their searches are not complete, but they tentatively find that such interactions do occur but only at temperature gradients and speeds too small to be physically interesting.

Let us return to the results shown in figure 6. We see that in addition to the weakly coupled convective and morphological instabilities predicted, Coriell *et al.* (1980) find a new mode, indicated by the dashed curve, which represents a time-periodic instability generated by the coupling of the two pure modes. For the lead–tin system, this time-periodic instability is not the first one to appear under ordinary operating conditions, though it can under extreme conditions of low G. S. R. Coriell (private communication) finds this to be the case for Pb–Sn when $G = 0.1$ K/cm and $V = 10$ μm/s. Schaefer & Coriell (1982) show for SCN–ethanol that the mode is present and can under ordinary conditions be preferred theoretically, as shown in figure 7 (though it was not observed in their experiment). These theoretical results are very interesting, but ones that caution the crystal grower. The 'attempt' to impress convective flow on a growing crystal may give rise to unwanted oscillations, rather than the homogenization that one sought.

The physical mechanism responsible for this oscillatory 'mixed' mode is not explained. However, consider the concentration field for the two uncoupled steady modes. The principal eigenfunction c of MI has maximum (minimum) concentration over the crests (troughs) of the interface corrugation as shown in figure 8(*a*). When

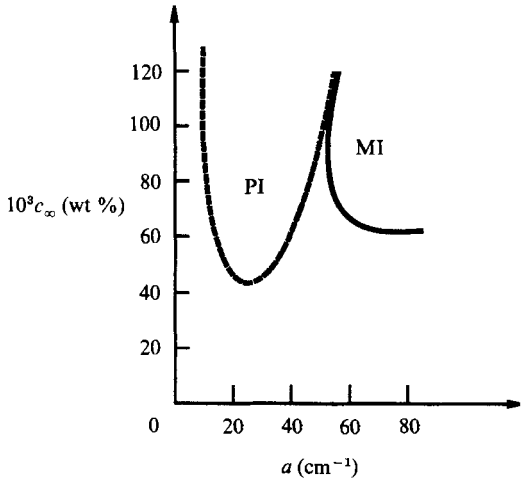

FIGURE 7. Neutral curves for SCN–ethanol for $V = 3\ \mu$m/s and $G = 10$ K/cm for upward solidification with the rejection of low-density solute. The steady morphological mode (solid line) and the time-periodic (PI) mixed mode (dashed line) are shown. The steady convective mode (CI) is not shown. Curves are taken from Schaefer & Coriell (1982).

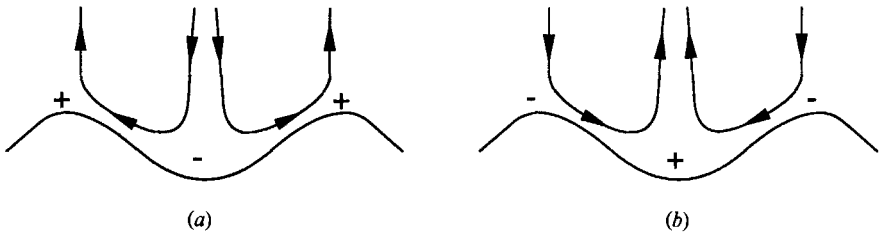

FIGURE 8. Sketch of eigenfunctions for linear stability theory for (*a*) morphological and (*b*) convective instabilities. The symbols + and − indicate signs of concentration perturbations at the interface.

buoyancy is present, and the solute Rayleigh number R is small, the low-density solute is transported laterally and will flow up the hills as shown in figures 8(*a*) and 9(*a*). When $R > R_c$, the situation reverses and the principal eigenfunction c involves vertical rises from the troughs and lateral transport that conserves mass. The eigenfunction of the convective instability modes would have the concentration elevated (depressed) above troughs (crests) as shown in figure 8(*b*). This picture has been verified by numerical calculation for one case by S. A. Forth & A. A. Wheeler (private communication). The two disturbance fields have competing concentration distributions and concommitant competing velocity distributions. At a wavenumber like $a \approx 140$ cm^{-1} in figure 6, where neither steady mode dominates, the oscillation might well flip back and forth between the two distributions, with the precise phasing among $\boldsymbol{v}$, c and h determining both the critical instability conditions and the frequency of oscillation. Such oscillatory states do occur in two-layer Bénard convection as described by Rasenet, Busse & Rehberg (1989).

For most common materials then $a_c^{(M)} \gg a_c^{(C)}$. However, there is the possibility that limiting cases exist which display a stronger coupling. Sivashinsky (1983) showed for the pure-morphological problem that, for $k \to 0$,

$$a_c^{(M)} \sim k^{\frac{1}{4}}. \tag{5.1}$$

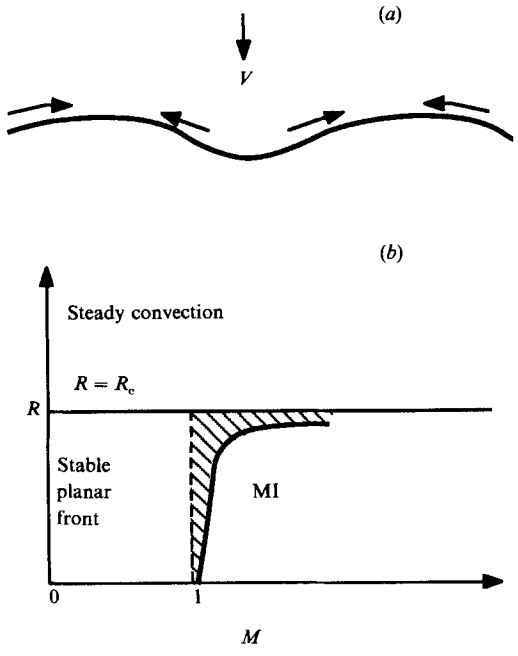

FIGURE 9. Upward solidification with rejection of low-density solute: (*a*) the lateral transport, (*b*) the linear-theory curves for asymptotically small-k materials. Curves are taken from Young & Davis (1986). The hatched area corresponds to the stabilization of MI by buoyancy.

Riley & Davis (1989*b*) show for the pure-convective problem that, for $k \to 0$,

$$a_c^{(C)} \sim k^{\frac{1}{4}}, \tag{5.2}$$

as well. Young & Davis (1986) examined the small-k limit for the coupled convective/morphological problem, and find a promising effect, as shown in figure 9(*b*). Above the line of Rayleigh number $R = R_c = 2(1+S^{-1})$ there is convective instability as shown by Hurle *et al.* (1982, 1983). However, there is another curve $R = R(M)$ to the right of which lies the region of MI as modified by buoyancy. Thus, for $R < R_c$, the morphological instability is delayed by buoyancy. This is an effect of lateral transport as discussed above as shown in figure 9(*a*). Consider the basic state perturbed initially by an interface corrugation. The rejected solute, if it is light, moves via a baroclinic motion, from troughs to crests, lowering the local $|G_c|$; there is an effective segregation coefficient produced, which has the value $k[1-(R/R_c)]^{-1}$ which is larger than k and gives an effectively smaller $|G_c|$. This delay of interfacial instability is a small one, but one of the new found to date.

The inability of workers to find beneficial couplings between morphological instability and buoyancy-driven convection has led some to examine simpler interactions in the hope that detailed understanding of coupling mechanisms will lead to effective control of morphological instability. Thus, rather than attempting to couple complex convective flows to the front, prescribed flows of different types have been examined. Apart from representing the 'poor man's convection', these flows can represent actual process conditions such as the effect of the rotation of the crystal. These topics are taken up now.

6. Forced flows

The study of forced flows over solidifying interfaces aims at understanding how the solute redistribution by the flow alters morphological instabilities or creates new instabilities. Further, forced flows serve as a surrogate, allowing one to isolate certain effects of convection in the melt and focusing on one-way couplings.

The first studies of forced flows were those of Delves (1968, 1971) who imposed a Blasius boundary layer on the interface and used the locally parallel-flow approximation; in effect they examined wavelengths short compared to the spreading length of the boundary layer. Arguments of local parallelism led Coriell *et al.* (1984) to impose plane Couette flow upon the interface.

If one pictures an imposed flow across an interface at 'infinity' and allows the solidification to proceed, the interface acts as a porous boundary and the forced flow has the asymptotic-suction profile, a boundary-layer flow on the scale δ_v, the viscous boundary-layer thickness,

$$\delta_v = \nu/V. \tag{6.1}$$

The velocity component along the interface has the form

$$u \propto 1 - e^{-z/\delta_v}. \tag{6.2}$$

The linear-theory problem for profile (6.2) coupled with MI was examined by Forth & Wheeler (1989).

Given that the concentration and thermal boundary layers scale on δ_c and δ_T, there are three lengths involved in such problems.

When one has an organic mixture, then

$$\delta_c \ll \delta_T \ll \delta_v \tag{6.3a}$$

since $\delta_v/\delta_T = \nu/\kappa = P$, and the Prandtl number P is large. However, if one has a small-Prandtl-number metallic alloy, then

$$\delta_c \ll \delta_v \ll \delta_T. \tag{6.3b}$$

These inequalities are relevant when one considers disturbances of various wavelengths λ. The 'normal' situation described in §2 has $\lambda < \delta_c$ so that the thermal field and the velocity field can be represented in locally linear forms:

$$T = T_0 + Gz \tag{6.4a}$$

and

$$u \sim \frac{V}{\nu} z, \tag{6.4b}$$

the latter being the plane Couette flow considered by Coriell *et al.* (1984). However, when λ becomes large enough, these localizations are no longer valid since the disturbances are affected by the curvature of the profiles. As discussed in §2, the distance L^+ from the interface to the upper heat source is a relevant lengthscale as well.

Coriell *et al.* (1984) and Forth & Wheeler (1989) find that MI is delayed by two-dimensional disturbances; these propagate with the flow. On the other hand disturbances in the form of longitudinal rolls decouple from the MI. Thus, under normal operating conditions parallel flows do not alter the critical conditions for MI. They only serve to select a preferred mode, longitudinal rolls, since these have the smallest V_c. Neither of these analyses examine those limiting cases that lead to long-wave MI. Forth & Wheeler do find small-wavenumber modes that can promote MI

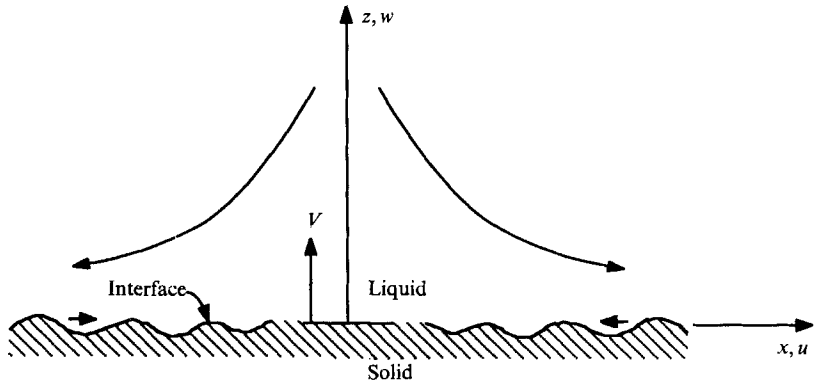

FIGURE 10. Two-dimensional stagnation-point (Hiemenz) flow impressed upon a solidifying interface. The waves on the interface propagate towards the stagnation point.

and involve propagation of waves against the flow. However, they do not identify conditions under which they are preferred.

Most imposed flows are not parallel. These range from the von Kármán swirl flow generated by the rotation of the crystal to the locally hyperbolic flows present when cellular convection exists at the interface.

Brattkus & Davis (1988*b*, *c*) studied flows with hyperbolic streamlines directed upon a solidifying interface. These were, respectively, a von Kármán swirl flow and stagnation-point flows. We discuss here the simplest of these, two-dimensional stagnation-point flow. Figure 10 shows the Hiemenz flow, which at $z = \infty$ has the form

$$u \sim (K\nu)^{\frac{1}{2}} x F'(z), \quad w \sim -(K\nu)^{\frac{1}{2}} F(z), \tag{6.5}$$

where F is a function that is known numerically and K measures the strength of the flow. The linear-stability problem is made tractable by assuming that the viscous-boundary-layer thickness δ_v is much larger than the concentration-boundary-layer thickness δ_c and that the Schmidt number S is very large. Explicitly, it is assumed that

$$\delta_c/\delta_v \equiv \left(\frac{D}{V}\right)\left(\frac{\nu}{K}\right)^{-\frac{1}{2}} = O(S^{-\frac{1}{3}}) \quad \text{as } S \to \infty. \tag{6.6}$$

Note that δ_v here is distinct from that in (6.1). Given the smallness of δ_c, the interface senses only the local forms of the imposed flow and the flow senses a flat interface; thus,

$$u \sim \beta x \zeta, \quad w \sim -\tfrac{1}{2}\beta \zeta^2, \tag{6.7}$$

where $\zeta = z/\delta_c$, and β measures $F''(0)$, the local shear. Finally, Brattkus & Davis considered waves long compared to δ_c though smaller than δ_v. They solved the modified diffusion problem

$$c_{\zeta\zeta}(1+\tfrac{1}{2}\beta\zeta^2)\, c_\zeta - \beta x \zeta c_x = c_\tau \quad (0 \leqslant \zeta < \infty), \tag{6.8a}$$

$$c_\zeta + (1-M^{-1})^{-1} c_\tau + [k(1-M^{-1})^{-1} + (1-k)]c = 0 \quad (\zeta = 0) \tag{6.8b}$$

$$c(\infty) = 0. \tag{6.8c}$$

Here $M = mG_c/G$ is the morphological number that measures constitutional undercooling, and τ is a scaled (slow) time. Note that the long-wave approximation leads to the neglect of the lateral diffusion term c_{xx}. This neglect is justified only far

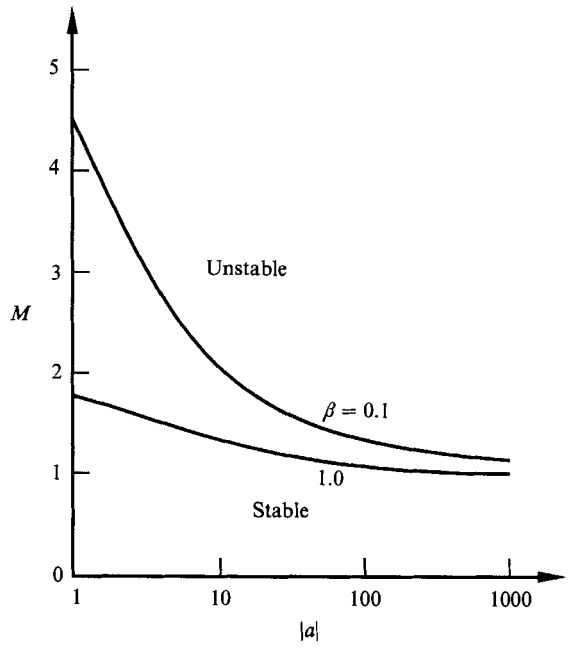

FIGURE 11. Neutral curve, M versus $|a|$, for long two-disturbances on a Hiemenz flow against a solidifying interface according to Brattkus & Davis (1988*c*) for $k = 0.3$. Here β is a non-dimensional measure of the shear stress exerted by the Hiemenz flow on the interface (Brattkus & Davis 1988*c*).

away from the stagnation point at $x = 0$ but makes tractable the solution of the linear-stability problem (6.8).

The non-parallel flow gives rise to the convective term xc_x that is scale invariant and so survives the long-wave approximation. The system (6.8) can be solved by employing quasi-normal modes as follows:

$$c(x, \zeta, \tau) = \mathrm{e}^{\sigma\tau + \mathrm{i}a \ln x} C(\zeta) \tag{6.9}$$

which converts system (6.8) into a constant-coefficient eigenvalue problem for growth rate $\sigma = \sigma(k, M; a)$. The system is solved numerically and figures 11 and 12 show the neutral curves and the frequency $\mathrm{Im}(\sigma)$ along the neutral curve.

The flow produces a long-wave instability that creates waves that travel inward, toward the stagnation point. The normal modes (6.9) are locally periodic in x but not globally so. The instability exists for long waves, in a region where the Mullins & Sekerka condition gives only stability. Thus, we call this *flow-induced morphological instability*. The largest growth rate $\mathrm{Re}(\sigma)$ occurs for $a \to \infty$ where the long-wave theory is invalid and where surface energy should help stabilize the interface. Thus, 'longish' waves would be preferred and these would grow for M just above unity, i.e. for any degree of constitutional undercooling; thus, it is a MI. The conjectured neutral stability curve, valid for all wavenumbers, would be as shown in figure 13. When the wavenumbers are large, the disturbances see only the local velocities and the flow appears to be locally parallel. The dashed curve of figure 13 shows the analogue of the results of Coriell *et al.* (1984) appropriate to locally parallel flows. When the wavenumbers are small, the disturbances see the curvature of the streamlines and hence the non-parallel-flow effects found by Brattkus & Davis (1988*c*), as shown in the solid curve of figure 13.

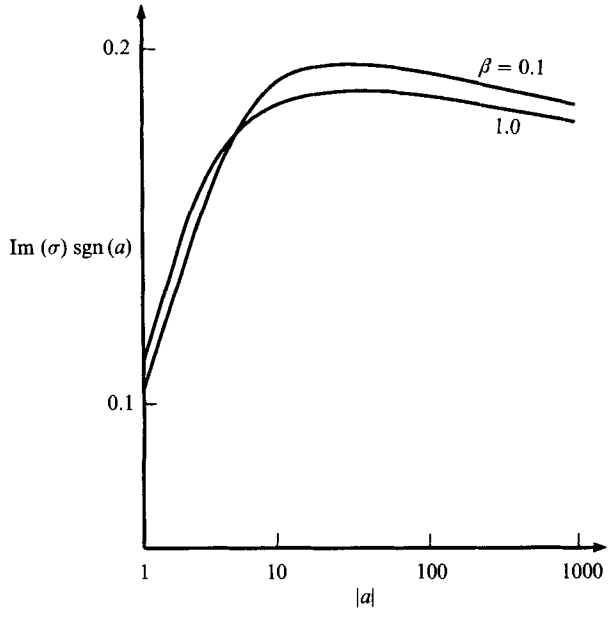

FIGURE 12. Disturbance angular frequency versus $|a|$ on the neutral curve for long two-dimensional disturbances on a Hiemenz flow against a solidifying interface according to Brattkus & Davis (1988*c*) for $k = 0.3$. Here β is a non-dimensional measure of the shear stress exerted by the Hiemenz flow on the interface (Brattkus & Davis 1988*c*).

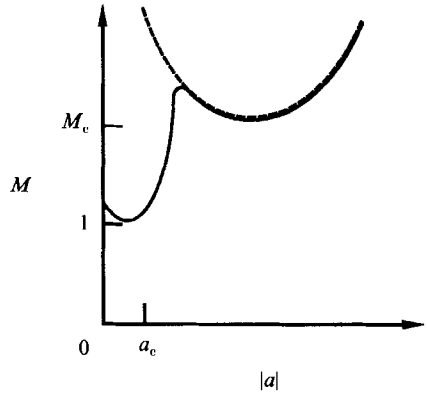

FIGURE 13. Conjectured neutral curve, M versus $|a|$, shown as the solid curve for general two-dimensional disturbances on a Hiemenz flow against a solidifying interface according to Brattkus & Davis (1988*b*). For small a, non-parallel effects dominate; for other a the curve coincides with the locally parallel theory of Coriell *et al.* (1984) as shown by the dashed curve.

The destabilization by non-parallel flow depends on both velocity components. The component normal to the mean position of the interface is directed inward. Its presence causes boundary-layer alteration. The concentration boundary layer is compressed, steepening the local gradient $|G_c|$. The lateral component of velocity (linear in x) varies with distance from the stagnation point and produces horizontal concentration gradients that drive the travelling cells that propagate into the oncoming flow. Brattkus & Davis (1988*b*) argue that these instabilities may be

responsible for the 'rotational striations' present in crystals produced in devices using crystal rotation.

The destabilization of long waves in the x-direction may be negated by 'end' effects that disallow the 'fitting' of such waves in the system. In this case the results of Coriell *et al.* (1984) would be regained. One could then allow disturbances of the form

$$c(y, z, t) = \mathrm{e}^{\sigma t + \mathrm{i}by} C(z) \tag{6.10}$$

for cross-stream periodic waves that are x-independent ($a = 0$). The full stagnation-point flow linear-stability problem has been examined in this case by McFadden, Coriell & Alexander (1988). They find that the flow slightly stabilizes MI.

The effects of unsteadiness in the melt flow have been investigated by Merchant & Davis (1989*a*). They consider plane stagnation-point flow against the interface but allow the flow at infinity to be time periodic, where the strength K of the flow in (6.5) is replaced by a time-periodic function as follows:

$$K \to K\Theta(\omega t) = K[1 + \delta \cos \omega t]. \tag{6.11}$$

They again consider long-wave two-dimensional disturbances and find that system (6.8) is replaced by the following:

$$c_{\zeta\zeta} + [1 + \tfrac{1}{2}\beta\Theta^{\frac{3}{2}}(\tau)\zeta^2]\, c_\zeta - \beta\Theta^{\frac{3}{2}}(\tau)\, x\zeta c_x = \gamma c_\tau, \tag{6.12a}$$

$$c_\zeta + \gamma(1 - M^{-1})^{-1} c_\tau + [k(1 - M^{-1})^{-1} + (1 - k)]\, c = 0 \quad (\zeta = 0), \tag{6.12b}$$

$$c(\infty) = 0, \tag{6.12c}$$

where

$$\gamma = \omega D / V^2 \tag{6.12d}$$

is the scaled forcing frequency. They find that modulation at low frequency stabilizes the interface against flow-induced morphological instabilities while high frequency promotes the instabilities. The response of the system to instability is quite complex with a disturbance being composed of two independent frequencies, the imposed frequency and the travelling-wave frequency modified by the modulation.

7. Flow over cells or dendrites

Consider the flow of magnitude U_0 over an isolated cell or dendrite tip of diameter d. If the flow is slow, so that the Reynolds number $Re = U_0 d/\nu \ll 1$, then the streamlines are symmetric front to back (upstream to downstream). However, the convection of solute may be substantial if the diffusivity D is small enough. Typically, D/ν is in the range 10^{-3} to 10^{-1} so that the Péclet number $Pe = U_0 d/D$ may be appreciable. In this case the isopycnals will not be symmetric since the flow sharpens the gradient in the front and weakens the gradient in the back. Given the steepened gradient in the front, the cell will modify its growth direction and will tilt into the shear flow; the front grows faster than the rear. This argument is due to Dantzig & Chao (1986) who verified this effect by experiment and by numerical simulation. This effect is not the result of an instability, but is due to boundary-layer alteration.

Consider now a row of such cells spaced along the flow direction. If the spacing is sufficiently large, the cells fail to 'interfere' with one another and the Dantzig/Chao effect will still tilt the cells flow-ward. As the spacing is decreased, 'interference' will occur and the tilting should be modified. These modifications may be related to the phenomena of MI/flow interactions discussed in §6. Brattkus & Davis (1988*b*, *c*)

found for non-parallel flows that long waves can produce a flow-induced MI that travels into the flow along the interface; presumably the nonlinear manifestation of this is the tilting of the cells. Now when conditions are such that wavelengths are not 'long', the instability waves will reverse the direction of propagation and the finite-amplitude cells might then alter their tilts. The possible relation between the flow over developed cells and interactive instabilities is intriguing.

A problem of vital interest to materials researchers is the coupling of convection with dendritic structures within and near the 'mushy' zone. The mushy zone is the two-phase region partially occupied by a field of dendrites (well above the MI threshold) and partially occupied by the interstitial fluid (enriched in solute). There are many models in which this zone is viewed as a porous material whose properties link dynamically with the overlying convective flow. The reader is referred to Huppert (1990) for an overview of these works.

8. Discussion

Unidirectional solidification is a means for the creation of phase change under controlled conditions. It is a vehicle for the study of the small-scale processes that determine the properties of the crystalline solid. At the interface latent heat is created and solute is rejected (or incorporated). These are diffused away from the interface and also convected by bulk motion of the liquid.

The mathematical description of such coupled systems typically involves fifteen or twenty parameters so that an understanding of the physics is necessary before one can even contemplate 'design'. Thus, in this paper we have emphasized physical mechanisms and have studied only the simplest systems available. Even then only a partial picture exists on how hydrodynamics and morphological changes couple. The discussion has emphasized mechanisms as a means of understanding, but also as a means of interesting experimentalists, who test the theories and identify new phenomena whose explanation would challenge the theoretician. The author knows of no quantitative experimental work on MI coupled to fluid flows. Recently de Cheveigné, Guthmann & Lebrun (1985, 1986), Eshelman & Trevedi (1987), and de Cheveigné *et al.* (1988) have tried to compare quantitatively experiments and theory on pure MI. The last of these finds discrepancies between critical wavelengths of cells which are partly attributable to the fact that the onset of instability occurs through a jump transition (at a subcritical bifurcation). However, Merchant & Davis (1989*b*) show on the basis of existing theories that supercritical bifurcation is experimentally accessible on the lower branch even with SCN-A.

To be sure experiments in this field are very delicate since for example one must know accurately the identities and levels of contaminants in the liquid. One must keep careful control on the thermal field and ensure that the concentration profiles (in the basic state) are time independent. All these things are necessary for the simplest model that we have described. There can as well be departures from this model intrinsic to the material. If the pulling speed V is too large for local thermodynamic equilibrium to apply, then kinetic effects may be present at the interface. Models of these exist (e.g. Coriell & Sekerka 1976); these lead to travelling waves on the interface in linear theory (Coriell & Sekerka 1976) and cells in the nonlinear range that tilt with respect to the growth direction (Young, Davis & Brattkus 1986). Further, if the surface energy γ of the interface is markedly anisotropic so that γ depends on crystalline orientation, then strong tilting of the cells can occur as well (Heslot & Libchaber 1985). Thus, both the choice of material

and the range of operation can be crucial. Nonetheless, the opportunity exists for good fluid-mechanical experimentation in hydrodynamically–morphologically coupled systems.

I am pleased to dedicate this article to George Batchelor, whose uncompromising standard of excellence is a model for us all.

This article has benefitted greatly from the suggestions of several individuals: K. Brattkus, R. J. Braun, S. R. Coriell, H. E. Huppert, G. J. Merchant, D. S. Riley and M. G. Worster. The author is indebted to S. A. Forth and A. A. Wheeler for undertaking the computation discussed in §5. He greatly appreciates the efforts of his secretary, Judy Piehl, who types what is meant rather than what is written, and the research support of the National Aeronautics and Space Administration, Microgravity Science and Applications Program.

REFERENCES

Alexander, J. I. D., Wollkind, D. J. & Sekerka, R. F. 1986 *J. Cryst. Growth* **79**, 849.

Boettinger, W. J., Shechtman, D., Schaefer, R. J. & Biancaniello, F. S. 1984 *Metall. Trans.* **15A**, 55.

Brattkus, K. 1988 Directional solidification of dilute binary alloys. Ph.D. Dissertation, Northwestern University.

Brattkus, K. & Davis, S. H. 1988*a* *Phys. Rev.* **B38**, 11452.

Brattkus, K. & Davis, S. H. 1988*b* *J. Cryst. Growth* **87**, 385.

Brattkus, K. & Davis, S. H. 1988*c* *J. Cryst. Growth* **89**, 423.

Brown, R. A. 1988 *AIChE J.* **34**, 881.

Caroli, B., Caroli, C., Misbah, C. & Roulet, B. 1985*a* *J. Phys. Paris* **46**, 401.

Caroli, B., Caroli, C., Misbah, C. & Roulet, B. 1985*b* *J. Phys. Paris* **46**, 1657.

Cheveigné, S. de, Guthmann, C., Kurowski, P., Vicente, E. & Biloni, H. 1988 *J. Cryst. Growth* **93**, 616.

Cheveigné, S. de, Guthmann, C. & Lebrun, M. M. 1985 *J. Cryst. Growth* **73**, 242.

Cheveigné, S. de, Guthmann, C. & Lebrun, M. M. 1986 *J. Phys. Paris* **47**, 2095.

Coriell, S. R., Cordes, M. R., Boettinger, W. S. & Sekerka, R. F. 1980 *J. Cryst. Growth* **49**, 13.

Coriell, S. R., McFadden, G. B., Boisvert, R. F. & Sekerka, R. F. 1984 *J. Cryst. Growth* **69**, 514.

Coriell, S. R., McFadden, G. B. & Sekerka, R. F. 1985 *Ann. Rev. Mater. Sci.* **15**, 119.

Coriell, S. R. & Sekerka, R. F. 1976 *J. Cryst. Growth* **34**, 157.

Dantzig, J. A. & Chao, L. S. 1986 *Proc. 10th US Natl Cong. Appl. Mech., Austin*, p. 249. ASME.

Delves, R. T. 1968 *J. Cryst. Growth* **3/4**, 562.

Delves, R. T. 1971 *J. Cryst. Growth* **8**, 13.

Eshelman, M. A. & Trevedi, R. 1987 *Acta Metall.* **35**, 2443.

Forth, S. A. & Wheeler, A. A. 1989 *J. Fluid Mech.* **202**.

Heslot, F. & Libchaber, A. 1985 *Physica Scr.* **T9**, 126.

Huppert, H. E. 1990 *J. Fluid Mech.* **212**, 209.

Hurle, D. T. J., Jakeman, E. & Wheeler, A. A. 1982 *J. Cryst. Growth* **58**, 163.

Hurle, D. T. J., Jakeman, E. & Wheeler, A. A. 1983 *Phys. Fluids* **26**, 624.

Jenkins, D. R. 1985 *IMA J. Appl. Maths* **35**, 145.

Langer, J. S. 1980 *Rev. Mod. Phys.* **52**, 1.

McFadden, G. B., Boisvert, R. F. & Coriell, S. R. 1987 *J. Cryst. Growth* **84**, 371.

McFadden, G. B., Coriell, S. R. & Alexander, J. I. D. 1988 *Commun. Pure Appl. Maths* **41**, 683.

MERCHANT, G. J. & DAVIS, S. H. 1989*a* *J. Cryst. Growth* **96**, 737.

MERCHANT, G. J. & DAVIS, S. H. 1989*b* *Phys. Rev. Lett.* **63**, 573.

MERCHANT, G. J. & DAVIS, S. H. 1989*c* Directional solidification near minimum c_∞: two-dimensional isolas and multiple solutions. *Phys. Rev. B* (1 December issue).

MULLINS, W. W. & SEKERKA, R. F. 1964 *J. Appl. Phys.* **35**, 444.

NOVICK-COHEN, A. & SIVASHINSKY, G. I. 1986 *Physica* **20D**, 237.

RASENAT, S., BUSSE, F. H. & REHBERG, I. 1989 *J. Fluid Mech.* **199**, 519.

RILEY, D. S. & DAVIS, S. H. 1989*a* *Applied Mathematics Tech. Rep.* 8838. Northwestern University.

RILEY, D. S. & DAVIS, S. H. 1989*b* Hydrodynamic stability of the melt during the solidification of a binary alloy with small segregation coefficient. *Physica* D (in press).

RILEY, D. S. & DAVIS, S. H. 1990 Long-wave morphological instabilities in the directional solidification of a dilute binary mixture. *SIAM J. Appl. Maths* (Spring 1990, pending publication).

ROSENBERGER, F. 1979 *Fundamentals of Crystal Growth I.* Springer.

RUTTER, J. W. & CHALMERS, B. 1953 *Can. J. Phys.* **31**, 15.

SCHAEFER, R. J. & CORIELL, S. R. 1982 In *Materials Processing in the Reduced Gravity Environment of Space* (ed. G. E. Rindone), p. 479. Mat. Res. Soc. Symp. Proc. North-Holland.

SIVASHINSKY, G. I. 1983 *Physica* **8D**, 243.

SRIRANGANATHAN, R., WOLLKIND, D. J. & OULTON, D. B. 1983 *J. Cryst. Growth* **62**, 265.

TILLER, W. A., JACKSON, K. A., RUTTER, J. W. & CHALMERS, B. 1953 *Acta-Metall.* **1**, 428.

TREVEDI, R., SEKHAR, J. A. & SEETHARAMAN, V. 1989 *Met. Trans.* **20A**, 769.

UNGAR, L. H., BENNETT, M. J. & BROWN, R. A. 1985 *Phys. Rev.* **B31**, 5923.

UNGAR, L. H. & BROWN, R. A. 1984*a* *Phys. Rev.* **B29**, 1367.

UNGAR, L. H. & BROWN, R. A. 1984*b* *Phys. Rev.* **B30**, 3993.

WOLLKIND, D. J. & SEGEL, L. A. 1970 *Phil. Trans. R. Soc. Lond.* A **268**, 351.

WOLLKIND, D. J., SRIRANGANATHAN, R. & OULTON, D. B. 1984 *Physica* **12D**, 215.

YOUNG, G. W. & DAVIS, S. H. 1986 *Phys. Rev.* **B34**, 3388.

YOUNG, G. W., DAVIS, S. H. & BRATTKUS, K. 1986 *J. Cryst. Growth* **83**, 560.